Eur Biophys J (2004) 33: 386–395
DOI 10.1007/s00249-003-0371-2

ARTICLE

Wolfgang Erker · Rüdiger Hübler · Heinz Decker

Structure-based calculation of multi-donor multi-acceptor fluorescence resonance energy transfer in the 4×6-mer tarantula hemocyanin

Received: 8 April 2003 / Revised: 19 July 2003 / Accepted: 14 October 2003 / Published online: 4 December 2003

Abstract Hemocyanins are oxygen carriers of arthropods and molluscs. The oxygen is bound between two copper ions, forming a Cu(II)-O_2^{2-}-Cu(II) complex. The oxygenated active sites create two spectroscopic signals indicating the oxygen load of the hemocyanins: first, an absorption band at 340 nm which is due to a ligand-to-metal charge transfer complex, and second, a strong quenching of the intrinsic tryptophan fluorescence, the cause of which has not been definitively identified. We showed for the 4×6-mer hemocyanin of the tarantula *Eurypelma californicum* that the fluorescence quenching of oxygenated hemocyanin is caused exclusively by fluorescence resonance energy transfer (FRET). The tarantula hemocyanin consists of 24 subunits containing 148 tryptophans acting as donors and 24 active sites as acceptors. The donor–acceptor distances are determined on the basis of a closely related crystal structure of the horseshoe crab *Limulus polyphemus* hemocyanin subunit II (68–79% homology). Calculation of the expected fluorescence quenching and the measured transfer efficiency coincided extraordinary well, so that the fluorescence quenching of oxygenated tarantula hemocyanin can be completely explained by Förster transfer. This results explain for the first time, on a molecular basis, why fluorescence quantum yield can be used as an intrinsic signal for oxygen load of at least one arthropod hemocyanin, in particular that from the tarantula.

Keywords Fluorescence quenching · Tryptophan · FRET · Oxygen binding · Tarantula hemocyanin

W. Erker (✉) · R. Hübler · H. Decker
Institute for Molecular Biophysics,
Johannes Gutenberg University,
Jakob Welder Weg 26,
55128 Mainz, Germany
E-mail: erker@biophysik.biologie.uni-mainz.de
Tel.: +49-6131-3923568
Fax: +49-6131-3923557

Introduction

Hemocyanins (Hc) are respiratory proteins of arthropods and molluscs, and are freely dissolved in the hemolymph (Salvato and Beltramini 1990; Markl and Decker 1992; Van Holde and Miller 1995; Van Holde et al. 2001). The hemocyanins of molluscs form high mass cylinders and reversibly bind up to 160 molecules of oxygen. The hemocyanins of arthropods occur as multiples of hexamers (1×6, 2×6, 3×6, 4×6, 6×6, 8×6). Each subunit, with a molar mass of about 72 kg/mol, reversibly binds one molecule of oxygen (Magnus et al. 1994). Although the structures of mollusc and arthropod hemocyanins are different, they have almost identical active sites. The active site of deoxygenated hemocyanins consists of two copper ions, Cu(I), each ligated by three histidines (Gaykema et al. 1984; Volbeda and Hol 1989; Hazes et al. 1993; Magnus et al. 1994). Oxygen is bound in a side-on (μ-η^2:η^2) coordination between the two ions (Kitajima et al. 1989, 1992; Baldwin et al. 1992; Magnus et al. 1994). Bound oxygen becomes a peroxide, oxidizing the copper ions to Cu(II).

For our investigation, the 4×6-mer hemocyanin of the tarantula *Eurypelma californicum* was used as a paradigm (Fig. 1). This 24-subunit hemocyanin contains seven different subunit types (*a*–*g*) (Markl et al. 1981). Each hexamer contains the subunits *a*, *d*, *e*, *f*, *g* and either the subunits *b* or *c*. Two of the four hexamers in the native hemocyanin contain the subunit *b*, the remaining two the subunit *c* (Fig. 1a). The tarantula hemocyanin contains 148 tryptophans and 24 active sites (Voit et al. 2000). Depending on the subunit type, the subunits contain five to eight tryptophans, with most of them located close to the active site (Fig. 1b) (Boteva et al. 1993). The 4×6-mer hemocyanin is composed of four hexamers, which look very similar to the hexamer structure of *Limulus polyphemus* subunit II hemocyanin obtained by electron microscopy (Van Heel and Dube 1994). In addition, the close relationship between the seven sequenced subunit types of the tarantula

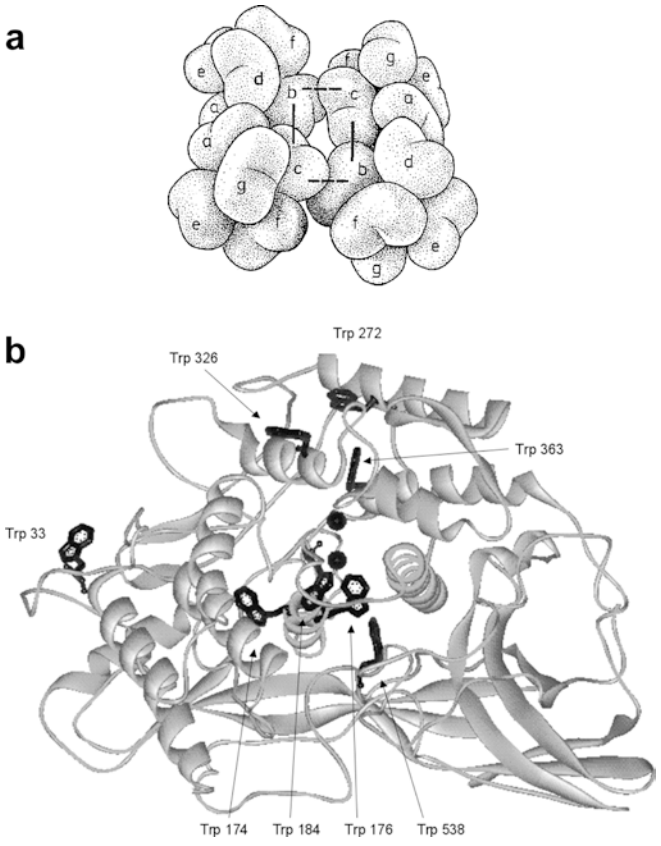

Fig. 1a, b Structure of *Eurypelma californicum* hemocyanin. (**a**) Quarternary structure. The 4×6-mer tarantula hemocyanin is composed of seven different subunit types (*a–g*) (Markl et al. 1981). Each subunit contains one active site. The 24 subunits are arranged in four hexamers. Each hexamer comprises subunits *a*, *d*, *e*, *f*, *g* and either subunit *b* or *c*. The two hexamers containing subunits *b* and *c* form a dodecamer. Two of these 12-mers associate to form the native protein [figure adapted from Savel-Niemann et al. (1988)]. (**b**) Subunit *g*. For illustration, the sequence of *Eurypelma* hemocyanin subunit *g* was modeled on the X-ray structure of deoxygenated *Limulus polyphemus* hemocyanin subunit II (Voit et al. 2000). The backbone of the protein is shown in *grey*, the two copper ions of the active site and the eight tryptophans are shown in *black*. The numbering of the eight tryptophan residues corresponds to the sequence of subunit II of the *Limulus polyphemus* hemocyanin (Magnus et al. 1994)

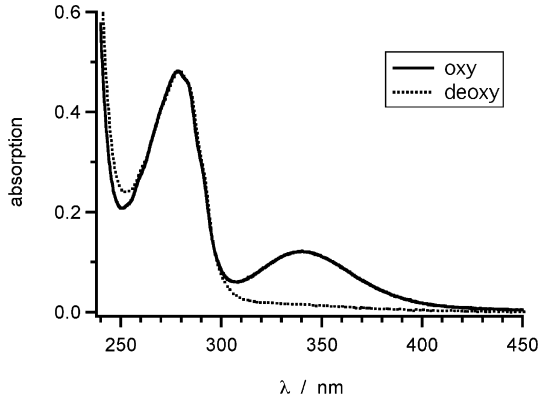

Fig. 2 Absorption spectra of 4×6-mer tarantula hemocyanin. Measurements were performed with hemocyanin at a concentration of $c = 0.44$ mg/mL in 100 mM Tris buffer, pH 7.8, containing 5 mM $CaCl_2$ and 5 mM $MgCl_2$, at 20 °C: oxygenated (*solid line*), deoxygenated (*dotted line*)

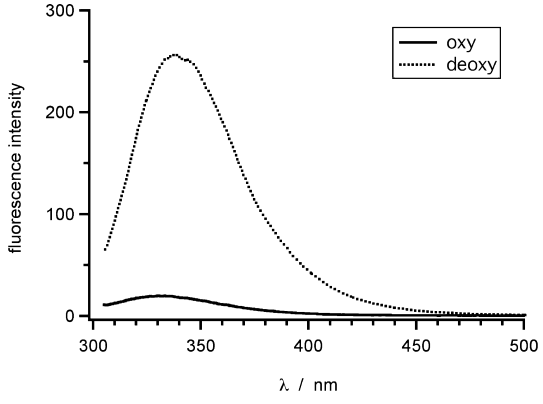

Fig. 3 Fluorescence emission spectra of 4×6-mer tarantula hemocyanin. Measurements were performed with hemocyanin at a concentration of $c = 0.1$ mg/mL in 100 mM Tris buffer, pH 7.8, containing 5 mM $CaCl_2$ and 5 mM $MgCl_2$, at 20 °C: oxygenated (*solid line*), deoxygenated (*dotted line*). The fluorescence of the intrinsic tryptophans was excited at a wavelength of $\lambda_{ex} = 295$ nm with a bandwidth of 5 nm. All spectra were corrected both for excitation and emission

hemocyanin and subunit II of the horseshoe crab hemocyanin is clear from the high sequence homology of 68–79% (Voit et al. 2000). The arrangement of the four hexamers in the native 4×6-mer has been revealed by electron microscopy (De Haas and Van Bruggen 1994).

The binding of oxygen to the active sites of hemocyanins is characterized by two spectroscopic signals. First, the two copper ions and the two oxygen atoms form a ligand-to-metal charge transfer complex with an absorption band at 340 nm and a molar extinction coefficient of $\epsilon_m(340\text{ nm}) = 20{,}000\ M^{-1}\ cm^{-1}$ (Fig. 2) (Salvato and Beltramini 1987; Magnus et al. 1994; Floyd et al. 2001). A linear relationship between the oxygen load and the absorption at 340 nm was shown by Richey et al. (1983). As a second signal, strong quenching of the intrinsic tryptophan fluorescence has been found (Fig. 3), with a linear dependency on the absorption at 340 nm (Shaklai and Daniel 1970; Loewe 1978). Thus, both the absorption and the fluorescence quenching can be used to monitor the oxygen load of hemocyanins.

The reason for the fluorescence quenching upon oxygen binding was investigated for molluscan hemocyanins and discussed controversially. Shaklai and Daniel (1970, 1972) assumed fluorescence resonance energy transfer between the tryptophans and the active sites. The tryptophans should act as donors, radiationlessly transferring their excitation energy to the oxygenated active sites. This idea was supported by the fact that, for hemocyanin of the snail *Levantina hierosolima*, the absorption band around 340 nm and the tryptophan fluorescence with a maximum at 336 nm had a large overlap, a condition necessary for Förster transfer (see below). Their calculated Förster radius of $R_0 = 3.0$ nm

appeared to be compatible with this mechanism, but a more detailed analysis of the observed efficiency of quenching in terms of this transfer was not possible because of missing structural data at that time. The investigations of Ricchelli et al. (1987) were interpreted as disproving this hypothesis. They analysed the fluorescence quenching of *Octopus vulgaris* hemocyanin for three different ligands bound to the active site, and concluded that a process other than Förster transfer must be responsible for at least some of the oxygen-dependent quenching. However, we will show that their conclusions were not correct.

The study reported here shows, at atomic level resolution, that Förster transfer is responsible for the oxygen-dependent quenching of the tryptophan fluorescence. The tryptophans are indeed able to transfer their energy to the oxygenated active sites. The multi-donor multi-acceptor quenching has been computed making use of the X-ray structure and the results compare very well with the measured values.

Material and methods

Hemocyanin preparation

Hemolymph of the tarantula *Eurypelma californicum* was obtained by dorsal puncture of the heart. All samples were diluted immediately 1:2 (v/v) with 0.1 M Tris/HCl buffer, pH 7.8, containing 5 mM $CaCl_2$ and 5 mM $MgCl_2$ in order to stabilize the protein. The samples were then centrifuged for 30 min at 13,000×*g* to remove blood cells. The hemocyanin was purified by gel filtration (Biogel A5m; 0.1 M Tris/HCl buffer, pH 7.8, containing 5 mM $CaCl_2$, 5 mM $MgCl_2$, at 20 °C). The large leading peak contained purified 4×6-mer hemocyanin, as supported by UV spectroscopy and two-dimensional immuno-gel electrophoresis.

Tarantula hemocyanin has an oxygen partial pressure at half saturation of $p_{50} = 12$ Torr; thus in air ($pO_2 = 160$ Torr) it is fully oxygenated. For deoxygenation, the hemocyanin solution was spread on a watch-glass and incubated for 1.5 h in a nitrogen atmosphere (Atmosbag, Sigma). The oxygen partial pressure of $pO_2 = 2.3$ Torr attained was low enough to obtain effectively complete deoxygenation in this highly cooperative oxygen-binding protein (Loewe 1978). Successful deoxygenation was tested by the absence of the absorption band at 340 nm (Fig. 2).

Absorption and fluorescence measurements

Hemocyanin absorption was measured in a semi-micro cuvette with a Hitachi U-3000 spectrophotometer, and the fluorescence with a Hitachi F-4500 spectrofluorimeter. All fluorescence spectra were corrected both for excitation and emission. The sample temperature was adjusted to 20 °C, if not otherwise indicated. To determine the quantum yields, 1 mM tryptophan in Tris buffer, pH 7.0, was chosen as the reference, with quantum yield $\Phi_R = 0.13$ (Chen 1967). This reference measurement alone was performed at 23 °C (Chen 1967). Emission spectra of hemocyanin and reference solutions excited at a wavelength of 295 nm (bandwidth 5 nm) were measured (bandwidth 5 nm) at different concentrations in the range between 0.025 mg/mL and 0.1 mg/mL in the case of hemocyanin and in the range between 20 μM and 200 μM in the case of tryptophan. For both samples there was a significant spectral overlap between scattered excitation light and fluorescence. As a result, the wavelength region below 305 nm of the emission spectra could not accurately be determined. To approximate this region of the spectra, the well-determined regions above 305 nm were each fitted with two Gaussian functions and the short-wavelength region extrapolated from there. The final spectra were integrated, standardized to their absorbance at 295 nm (A_{295}) and corrected for the inner filter effect at the excitation wavelength (Lakowicz 1999):

$$F(\lambda) = F_{\text{measured}}(\lambda) \times 10^{\frac{\text{Abs}_{295}}{2}} \quad (1)$$

The inner filter effect at the emission wavelength was negligible because of the much lower absorption due to the shorter light path in observation (1 mm). Based on the corrected spectra $F(\lambda)$, the quantum yields (Φ) were calculated from the integrated spectra F according to: $\Phi/\Phi_R = F/F_R$.

The overlap integral was calculated with Eq. (2), below, based on the final emission spectrum of deoxygenated hemocyanin (see above) and the absorption spectrum of the oxygenated active sites around 340 nm. To take into account of the overlap between the absorption band of the protein around 280 nm and that of the active sites at 340 nm (Fig. 2), the 340 nm band was fitted with a single Gaussian function in the range 305–500 nm and the spectra at shorter wavelengths extrapolated from that. The fitted absorption spectrum was transferred into a spectrum of the molar extinction coefficient $\epsilon_m(\lambda)$ using the Lambert–Beer law: $A(\lambda) = \epsilon_m(\lambda) \times c \times d$, where c is the molar concentration of solute and d the pathlength. The hemocyanin concentration was determined using an extinction coefficient at 278 nm of $\epsilon(278\text{ nm}) = 1.1\text{ (mg/mL cm)}^{-1}$ (Loewe 1978) and a molar mass of 1.72×10^6 g/mol for the 4×6-mer (Voit et al. 2000), containing 24 oxygen binding sites.

Distances between the tryptophans and the active sites

The distances (r_{ij}) between the tryptophans and the active sites within the hemocyanin of *Eurypelma californicum* were determined on the basis of the X-ray structure of oxygenated subunit II of *Limulus polyphemus* hemocyanin (Protein Data Bank, http://www.rcsb.org/pdb/cgi/explore.cgi?pid=23641069670174&page=0&pdbId=1OXY) (Magnus et al. 1994). The sequence alignment was taken from Voit et al. (2000) to determine the homologous positions of tryptophans in *Limulus polyphemus* hemocyanin. For tryptophan residues which were not conserved, the amino acids of the homologous positions were used. The distances between the $C_{\delta 2}$ positions of the tryptophans and the center between the two copper atoms of the active site were measured. The arrangement of the four hexamers in the native 4×6-mer was taken as that solved by electron microscopy (De Haas and Van Bruggen 1994) and later modified for oxygenated tarantula hemocyanin by SAXS measurements (Decker et al. 1996; Hartmann and Decker 2002). For calculating the fluorescence quenching within the 4×6-mer, the distances between every 148 tryptophans and each of the 24 active sites were considered.

Theory

Förster energy transfer

Excited dyes (donors) may transfer their energy radiationlessly to an adjacent chromophore (acceptor) (Förster 1948). For transfer processes of this type, an overlap between the emission spectrum of the donor and the absorption spectrum of the acceptor is necessary. The amount of overlap is expressed by the overlap integral J ($\text{nm}^4\ \text{M}^{-1}\ \text{cm}^{-1}$) (Fairclough and Cantor 1978; Stryer 1978; Van der Meer et al. 1994):

$$J = \frac{\int F(\lambda)\varepsilon_m(\lambda)\lambda^4 \mathrm{d}\lambda}{\int F(\lambda)\mathrm{d}\lambda} \quad (2)$$

where $F(\lambda)$ is the fluorescence intensity of the donor in absence of the acceptor per unit wavelength interval at wavelength λ, and $\epsilon_m(\lambda)$ the molar extinction coefficient ($\text{M}^{-1}\ \text{cm}^{-1}$) of the acceptor at

wavelength λ. Förster transfer is based on a dipole–dipole coupling mechanism which is strongly distance dependent. The proportion of excited donors transferring their energy to an acceptor is given by the transfer efficiency E:

$$E = \frac{R_0^6}{R_0^6 + r^6} \tag{3}$$

where r is the distance between donor and acceptor and R_0 (nm) is the distance where half of the excited molecules relax into the ground state via Förster transfer. This critical or Förster distance can be calculated by (Van der Meer et al. 1994):

$$R_0^6 = 8.79 \times 10^{-11}\ (\mathrm{nm^2\ M\ cm}) \times \frac{\Phi_0 J \kappa^2}{n^4} \tag{4}$$

Here, Φ_0 is the quantum yield in the absence of Förster transfer and n the refractive index of the medium between donor and acceptor. κ^2 is the orientation factor, describing the relative orientation of the transition dipole moments of the donor and the acceptor.

Multi-donor multi-acceptor systems

The quantum yield Φ_0 of a single fluorophore in absence of a Förster transfer acceptor is given by:

$$\Phi_0 = \frac{k_F}{k_F + k_R} \tag{5}$$

where k_F and k_R are the rate constants of fluorescence emission and of all other processes, respectively, which are responsible for the depopulation of the excited state. In the event of an additional quenching process with rate constant k_Q, the quantum yield has the form:

$$\Phi = \frac{k_F}{k_F + k_R + k_Q} = \frac{1}{\frac{1}{\Phi_0} + \frac{k_Q}{k_F}} \tag{6}$$

In the case of Förster transfer, the quenching constant rate k_Q can be written as (e.g., Lakowicz 1999):

$$k_Q = \frac{1}{\tau_0}\left(\frac{R_0}{r}\right)^6 \tag{7}$$

Here, R_0 is the Förster distance given by Eq. (4), r the distance between donor and acceptor, and τ_0 the excited state lifetime of the donor in the absence of the acceptor:

$$\tau_0 = \frac{1}{k_F + k_R} \tag{8}$$

From the Eqs. (7), (8) and (5) one obtains:

$$\frac{k_Q}{k_F} = \frac{1}{\Phi_0}\left(\frac{R_0}{r}\right)^6 \tag{9}$$

and the quantum yield of a fluorophore quenched by Förster transfer (Eq. 6) becomes:

$$\Phi = \frac{\Phi_0}{1 + \left(\frac{R_0}{r}\right)^6} \tag{10}$$

For a system of D otherwise equivalent donors with different distances r_i to a single acceptor this becomes:

$$\Phi = \frac{1}{D}\sum_{i=1}^{D}\Phi_i = \frac{1}{D}\sum_{i=1}^{D}\frac{\Phi_0}{1 + \left(\frac{R_0}{r_i}\right)^6} \tag{11}$$

In contrast, when the system consists of a single donor and A acceptors with different constant rates k_{Qj}, Eq. (6) changes to:

$$\Phi = \frac{k_F}{k_F + k_R + \sum_{j=1}^{A} k_{Qj}} = \frac{1}{\frac{1}{\Phi_0} + \sum_{j=1}^{A}\frac{k_{Qj}}{k_F}} \tag{12}$$

This equation describes the competition of different quenching processes. Inserting Eq. (9) yields instead of Eq. (10) a quantum yield of:

$$\Phi = \frac{\Phi_0}{1 + \sum_{j=1}^{A}\left(\frac{R_0}{r_j}\right)^6} \tag{13}$$

where r_j is the distance between the donor and the A different acceptors. For the case that D donors are quenched by A acceptors, we obtain by inserting Eq. (13) in the middle term of Eq. (11):

$$\Phi = \frac{1}{D}\sum_{i=1}^{D}\frac{\Phi_0}{1 + \sum_{j=1}^{A}\left(\frac{R_0}{r_{ij}}\right)^6} \tag{14}$$

where r_{ij} is the distance between the donor i and the acceptor j. This derivation is based on the assumptions (1) that each and every donor has identical spectroscopic properties in absence of the acceptors, themselves having identical absorption properties, so that R_0 is the same for any donor, and (2) that only the occurrence of fluorescence resonance energy transfer (FRET) affects these properties in the presence of acceptors, i.e. the only parameters changed in presence of the acceptors being the donor lifetimes and, due to that, their quantum yields. There was previously a similar derivation by Dewey and Hammes (1980) for distributions of donors and acceptors on surfaces.

The degree of quenching, expressed by the transfer efficiency E, is given by (e.g., Lakowicz 1999):

$$E = 1 - \frac{\Phi}{\Phi_0} = 1 - \frac{I}{I_0} \tag{15}$$

where I and I_0 are the donor fluorescence intensities measured on the same sample fully oxygenated and fully deoxygenated, respectively.

Error propagation

In order to estimate the confidence interval of the calculated transfer efficiencies, one has to know the error range. For this the error propagation was applied for the multi-donor multi-acceptor case. In the middle term of Eq. (15), which is used for the calculations, the quantities Φ_0, J, κ^2, n and r_{ij} are all afflicted with errors (after inserting Eqs. 14 and 4). For an error estimation, one needs the partial derivatives of E with respect to these quantities:

1. Quantum yield:

$$\frac{\partial E}{\partial \Phi_0} = \frac{1}{D}\sum_{i=1}^{D}\frac{\frac{1}{\Phi_0}\sum_{j=1}^{A}\frac{R_0^6}{r_{ij}^6}}{\left(1 + \sum_{j=1}^{A}\frac{R_0^6}{r_{ij}^6}\right)^2} \tag{16}$$

2. Overlap integral:

$$\frac{\partial E}{\partial J} = \frac{1}{D}\sum_{i=1}^{D}\frac{\frac{1}{J}\sum_{j=1}^{A}\frac{R_0^6}{r_{ij}^6}}{\left(1 + \sum_{j=1}^{A}\frac{R_0^6}{r_{ij}^6}\right)^2} \tag{17}$$

3. Orientation factor:

$$\frac{\partial E}{\partial \kappa^2} = \frac{1}{D}\sum_{i=1}^{D} \frac{\frac{1}{\kappa^2}\sum_{j=1}^{A}\frac{R_0^6}{r_{ij}^6}}{\left(1+\sum_{j=1}^{A}\frac{R_0^6}{r_{ij}^6}\right)^2} \tag{18}$$

4. Refractive index:

$$\frac{\partial E}{\partial n} = \frac{1}{D}\sum_{i=1}^{D} \frac{-\frac{4}{n}\sum_{j=1}^{A}\frac{R_0^6}{r_{ij}^6}}{\left(1+\sum_{j=1}^{A}\frac{R_0^6}{r_{ij}^6}\right)^2} \tag{19}$$

5. Distances:

$$\frac{\partial E}{\partial r} = \sqrt{\sum_{i=1}^{D}\sum_{j=1}^{A}\left(\frac{\partial E}{\partial r_{ij}}\right)^2} = \sqrt{\sum_{i=1}^{D}\sum_{j=1}^{A}\left(\frac{-\frac{6}{D}\frac{R_0^6}{r_{ij}^7}}{\left(1+\frac{R_0^6}{r_{ij}^6}\right)^2}\right)^2} \tag{20}$$

The total error of the transfer efficiency E is given according to Gauss.

Results and discussion

Measurements

Absorbance and fluorescence emission spectra were obtained from oxygenated and deoxygenated 4×6-mer hemocyanin of the tarantula *Eurypelma californicum* (Figs. 2 and 3). The oxygen binding is accompanied by the appearance of an absorption band in the spectral region around 340 nm (Fig. 2) and a strong decrease of the fluorescence quantum yield (Fig. 3). The fluorescence quantum yields of the two forms were determined as $\Phi_0 = 0.0727 \pm 0.0073$ ($\pm 10\%$) for deoxygenated hemocyanin and $\Phi = 0.0055 \pm 0.0008$ ($\pm 15\%$) for oxygenated hemocyanin. Hence, the quantum yield drops by a factor of about 13. Deoxygenated hemocyanin has a lower relative error than oxygenated hemocyanin, because the intensity is 13× higher and therefore it could be determined more accurately. The measured quantum yields are in good agreement with those reported previously: Boteva et al. (1993) determined values of $\Phi_{deoxy} = 0.065$ and $\Phi_{oxy} = 0.006$, respectively. The differences between both studies are within the error range.

The maximum of the fluorescence emission spectrum of deoxygenated hemocyanin (340 nm, Fig. 3) coincides with the maximum of the oxygen-dependent absorption band of oxygenated hemocyanin (Fig. 2). In consequence, there is a strong overlap between the tryptophan fluorescence and the absorption band, making fluorescence quenching due to Förster transfer very probable. Nevertheless, the mechanism for the fluorescence quenching of hemocyanins upon oxygenation is still unclear.

Assuming FRET as the exclusive quenching mechanism, the measured results presented in this study correspond to a transfer efficiency of $E = 0.9243 \pm 0.0101$ (Eq. 15). The relative error of E ($\Delta E/E = 1.1\%$) is much smaller than the errors of the individual quantum yields (10% for deoxygenated and 15% for oxygenated hemocyanin) because of the strong quenching and because it does not contain the uncertainty of the reference ($\Delta\Phi/\Phi = 8\%$; Chen 1967). The results of Boteva et al. (1993) correspond to a transfer efficiency of $E = 0.908$, which is slightly smaller than that observed here.

Theoretical consideration of the quenching

The hypothesis that tryptophan quenching in the fully oxygenated hemocyanin is entirely due to Förster transfer was tested by calculating the transfer efficiency and comparing it with the measured one (Eq. 15). Hemocyanins contain many tryptophans which may act as donors and many active sites acting as potential acceptors. Therefore, describing the quantum yield by Eq. (10) is not sufficient because it describes the quenching of a single donor by a single acceptor. The expansion for multi-donor multi-acceptor systems which are quenched by Förster transfer is given by Eq. (14). The individual distances r_{ij} between acceptors and donors can be deduced from X-ray structures. However, it is not possible to determine the Förster distance R_0 (the values of Φ_0, J, κ^2 and n) for each donor–acceptor pair. Therefore, it has been assumed that these factors are identical for all donor–acceptor pairs, so that the average of the quantum yield of all donors in the quenched system can be represented by Eq. (14). This assumption is supported by the fact that tarantula hemocyanin contains 148 tryptophans and 24 active sites (Voit et al. 2000). There are 44 different tryptophan types within the seven different subunit types (Table 1). This means that there are 44×24 = 1056 different interactions between donors and acceptors. These numbers appear large enough to justify an ensemble approximation.

In principle, it should be possible to determine individual orientation factors for each donor–acceptor pair from the X-ray structure. The orientation of the transition dipole of an oxygenated active site is located on the axis connecting the copper ions (personal communication of Prof. Dr. F. Tuczek, Institute for Inorganic Chemistry, University of Kiel, Germany). However, to our knowledge the orientation of the transition dipole moment of tryptophan is not known. The orientation of the transition dipole moment of indole has been published by Callis (1997), who assumed that the orientation of the transition dipole moment of tryptophan is located

Table 1 Calculation of the quenching of tryptophan fluorescence within the seven subunit types of the tarantula hemocyanin. The numbering of the amino acids (column 2) corresponds to the sequence of subunit II of the *Limulus polyphemus* hemocyanin (Magnus et al. 1994). The *asterisk* (*) in column 2 indicates the trpytophan residues which are not conserved in tarantula hemocyanin with respect to the*Limulus*hemocyanin subunit II. For illustration, the distances between the tryptophans and the active sites of the *same* subunit are listed in column 4. The distances r_j were determined on the basis of the X-ray structure of oxygenated hemocyanin (subunit II) of *Limulus polyphemus*. The transfer efficiencies E of each individual tryptophan (column 5) were calculated with Eqs. (13) and (15) using $R_0 = 2.40$ nm. Thus, the transfer efficiencies listed in column 5 are attributed to the quenching of every tryptophan by *all* active sites within the 4×6-mer

Subunit	Trp no.	Atom	Distance within subunit, r_j (nm)	Total transfer efficiency, E
a	174	$C_{\delta 2}$	1.173	0.9865
	176	$C_{\delta 2}$	0.770	0.9989
	272*	S_{δ}	1.529	0.9385
	326	$C_{\delta 2}$	1.357	0.9686
	538	$C_{\delta 2}$	1.320	0.9731
b	174	$C_{\delta 2}$	1.173	0.9865
	176	$C_{\delta 2}$	0.770	0.9989
	184	$C_{\delta 2}$	1.681	0.8951
	326	$C_{\delta 2}$	1.357	0.9686
	363	$C_{\delta 2}$	0.916	0.9969
	538	$C_{\delta 2}$	1.320	0.9731
	612*	$C_{\delta 2}$	2.873	0.3133
c	174	$C_{\delta 2}$	1.173	0.9865
	176	$C_{\delta 2}$	0.770	0.9989
	184	$C_{\delta 2}$	1.681	0.8955
	272*	S_{δ}	1.529	0.9385
	326	$C_{\delta 2}$	1.357	0.9686
	363	$C_{\delta 2}$	0.916	0.9969
	538	$C_{\delta 2}$	1.320	0.9731
d	174	$C_{\delta 2}$	1.173	0.9865
	176	$C_{\delta 2}$	0.770	0.9989
	272*	S_{δ}	1.529	0.9385
	326	$C_{\delta 2}$	1.357	0.9686
	366*	$C_{\delta 2}$	1.186	0.9857
	538	$C_{\delta 2}$	1.320	0.9731
e	174	$C_{\delta 2}$	1.173	0.9865
	176	$C_{\delta 2}$	0.770	0.9989
	184	$C_{\delta 2}$	1.681	0.8947
	272*	S_{δ}	1.529	0.9384
	326	$C_{\delta 2}$	1.357	0.9686
	538	$C_{\delta 2}$	1.320	0.9731
f	174	$C_{\delta 2}$	1.173	0.9865
	176	$C_{\delta 2}$	0.770	0.9989
	184	$C_{\delta 2}$	1.681	0.8948
	272*	S_{δ}	1.529	0.9385
	538	$C_{\delta 2}$	1.320	0.9731
g	33*	C_{δ}	3.224	0.1555
	174	$C_{\delta 2}$	1.173	0.9865
	176	$C_{\delta 2}$	0.770	0.9989
	184	$C_{\delta 2}$	1.680	0.8947
	272*	S_{δ}	1.529	0.9385
	326	$C_{\delta 2}$	1.357	0.9686
	363	$C_{\delta 2}$	0.916	0.9969
	538	$C_{\delta 2}$	1.320	0.9731

within a range of $\pm 10°$ compared to that of indole. This uncertainty results in a large error of the orientation factor κ^2. The orientation factor is defined by (e.g., Van der Meer et al. 1994):

$$\kappa^2 = (\sin\delta \times \sin\alpha \times \cos\phi - 2\cos\delta \times \cos\alpha)^2 \qquad (21)$$

where δ is the angle between the transition dipole moment of the donor and the connection between donor and acceptor, α is the angle between the transition dipole moment of the acceptor and the connection between donor and acceptor, and ϕ is the angle between the planes determined by the connection vector and the transition dipole moments of donor and acceptor. Assuming arbitrary values of $\delta = 45°$, $\alpha = 45°$ and $\phi = 45°$, one obtains $\kappa^2(\delta = \alpha = \phi = 45°) = 0.418$. Including uncertainties of the three angles, $\Delta\delta = 10°$ (see above), $\Delta\alpha = 2°$ and $\Delta\phi = 2°$ (respecting differences between the structures of *Eurypelma* and *Limulus* hemocyanin) results in the two extreme values of $\kappa^2(\delta = 35°$, $\alpha = 43°$ and $\phi = 47°) = 0.868$ and $\kappa^2(\delta = 55°$, $\alpha = 47°$ and $\phi = 43°) = 0.118$, respectively. The deviations are quite large: a factor of 2.1 (0.868/0.418) for the upper limit and a factor of 3.5 (0.418/0.118) for the lower one. Therefore, the determination of individual orientation factors for every donor–acceptor pair would not increase the accuracy of our calculation. The knowledge of the orientation of the transition dipole moment of tryptophan is too uncertain for our purpose so far. Because of that, we used the commonly used value of $\kappa^2 = 2/3$ as an average for each donor–acceptor pair (Dos Remedios and Moens 1995; Lakowicz 1999).

For the computation of the Förster radius R_0 as a global parameter, according to Eq. (4), knowledge of the unquenched quantum yield Φ_0, the overlap integral J, the refractive index n and the orientation factor κ^2 is necessary. The quantum yield of deoxygenated hemocyanin was determined to be $\Phi_0 = 0.0727$ (see above). The overlap integral was calculated, based on the absorption and fluorescence spectra at different hemocyanin concentrations (examples are shown in Figs. 2 and 3), using Eq. (2) and yielded a value of $J = 1.72 \times 10^{14}$ nm^4 M^{-1} cm^{-1} ($\pm 7\%$). The error in J is an estimation respecting uncertainties concerning the knowledge of the molar extinction coefficient ϵ(340 nm) and our measurements. While the values of the quantum yield Φ_0 and the overlap integral J were determined experimentally, the values for the orientation factor κ^2 (2/3, see above) and the refractive index n were taken from the literature. For the refractive index a value of $n = 1.4$, commonly used for proteins, was applied (Van der Meer et al. 1994). With these values, Eq. (4) yields a Förster radius of $R_0 = 2.40 \pm 0.22$ nm for the 4×6-mer tarantula hemocyanin. This agrees well with the value published for the molluscan hemocyanin from *Octopus vulgaris*: $R_0 = 2.5$ nm (Ricchelli et al. 1987). Shaklai and Daniel (1970) published a larger Förster distance of $R_0 = 3.0$ nm for *Levantina hierosolima* hemocyanin.

Owing to the close relationship and high sequence homology of arthropodan hemocyanins, the structure of *Limulus polyphemus* hemocyanin (oxygenated form) was used to determine the distances r_{ij} between the tryptophans and the active sites in the 4×6-mer hemocyanin of *Eurypelma californicum* (Linzen et al. 1985; Hazes et al.

1993; Voit et al. 2000; Burmester 2001). The distances were measured between the $C_{\delta 2}$ positions and the center between the two copper atoms of the active site. The amino acids of the homologous position were used for tryptophan residues which were not conserved in tarantula hemocyanin with respect to *Limulus polyphemus* hemocyanin (labeled with an asterisk in Table 1, column 2). The distances between the tryptophans and the active site of the *same* subunit are listed in Table 1 (column 4). Because hemocyanins from arthropods form well-defined tertiary and quarternary structures (Markl and Decker 1992; Van Holde and Miller 1995), the distances between the donors and acceptors within the hemocyanin are considered constant, i.e. not to fluctuate appreciably at any relevant time scale.

With these assumptions, Eq. (15) with Eqs. (14) and (4) provides an average transfer efficiency of the quenched (oxygenated) 4×6-mer hemocyanin of $E = 0.9359$. This is in extraordinarily good agreement with the measured value of $E_{\text{measured}} = 0.9243$ (see above). In order to validate the calculated transfer efficiencies, an error propagation must be computed.

Error propagation

The total error of the calculated transfer efficiency E was determined presuming the following errors in the starting parameters: $\Delta\Phi_0/\Phi_0 = 10\%$, $\Delta J/J = 7\%$, $\Delta n/n = 5\%$ and $\Delta r = 0.02$ nm. The error for the quantum yield is rather high because of the uncertainty of the reference used ($\Delta\Phi_R/\Phi_R = 8\%$; Chen 1967). Because we were not able to determine the orientation factor for individual donor–acceptor pairs, as stated above, the error in the average value of κ^2 could be quite high. Therefore, the total error of E was calculated for different errors of the orientation factor in the range of $\Delta\kappa^2/\kappa^2 = 0$–$75\%$ (Table 2). The calculations show that even for large errors of the orientation factor the error of the transfer efficiency remains rather small (a few percent). Even though very high values for the average orientation factor were used, the computed transfer efficiency does not change very much. For example, repeating the calculation with a very large average orientation factor of $\kappa^2 = 3$ because an error propagation is not possible in that case, the transfer efficiency E just increases 4.0% compared to $E(\kappa^2 = 2/3) = 0.9359$. Consequently, the uncertainty of κ^2 has a negligible influence on the computed transfer efficiency. The computed transfer efficiency of $E = 0.9359 \pm 0.0201$ for $\Delta\kappa^2/\kappa^2 = 50\%$ fits extraordinarily well the measured one, $E_{\text{measured}} = 0.9243 \pm 0.0136$. This means that (1) the Förster transfer fully explains the fluorescence quenching in oxygenated tarantula hemocyanin, and (2) no other process is necessary to explain the quenching.

The total error ΔE is composed of five uncertainties: $\Delta\Phi_0 = 0.0036$, $\Delta J = 0.0026$, $\Delta\kappa^2 = 0.0182$ (assuming $\Delta\kappa^2/\kappa^2 = 50\%$), $\Delta n = 0.0073$ and $\Delta r = 0.0004$. Thus, ΔE is dominated by the error in κ^2, the contribution of n is minor and the contributions of Φ_0, J and r can be neglected.

Table 2 Total error of the calculated transfer efficiency E in dependance on the error in the orientation factor κ^2. The error in E (column 2), calculated according to Gauss with Eqs. (16)–(20), contains the uncertainties for Φ_0 (10%), J(7%), κ^2 (column 1), n (5%) and r_{ij} (0.02 nm). For computation the values $R_0 = 2.40$ nm, $\Phi_0 = 0.0727$, $J = 1.72\times10^{14}$ nm^4 M^{-1} cm^{-1}, $\kappa^2 = 2/3$ and $n = 1.4$ were used. The distances r_{ij} between the 148 donors and the 24 acceptors were determined on the basis of the X-ray structure of oxygenated hemocyanin (subunit II) of *Limulus polyphemus*

Error in the orientation factor $\Delta\kappa^2$(%)	Total error in the transfer efficiency ΔE (%)
0	0.9
25	1.3
50	2.2
75	3.1

Class distribution of the tryptophans

Because of the topological arrangement of the 4×6-mer tarantula hemocyanin (Fig. 1), equal tryptophans within different subunits of the same subunit type (*a*–*g*) are quenched by the 24 active sites to the same degree. The calculated transfer efficiencies of the tryptophans for all seven subunit types are listed in Table 1 (column 5). All tryptophans were quenched by more than 89%, except for two tryptophans. These two tryptophans are located in subunit *b* (Trp 612) and subunit *g* (Trp 33). Since subunit *b* occurs twice in the 4×6-mer and subunit *g* four times, there are only six tryptophans within the 4×6-mer hemocyanin which are quenched significantly less. In consequence, there are two classes of tryptophans consisting of six and 142 residues, respectively. Based on the calculation, the contribution of these six tryptophans to the total quantum yield of the oxygenated hemocyanin is $(2\times0.0499 + 4\times0.0614)/148 = 0.0023$ (transfer efficiencies were taken from Table 1, quantum yields calculated with Eq. 15). The calculated quantum yield of all 148 tryptophans within the oxygenated hemocyanin was determined to be $\Phi = 0.0047$. Thus, the six weakly quenched tryptophans account for 50% of the total fluorescence intensity of the oxygenated 4×6-mer.

Comparison with former studies

In the past, three groups have dealt with the origin of fluorescence quenching in oxygenated hemocyanins. While Shaklai and Daniel (1970, 1972) assumed Förster transfer to be responsible for the quenching, the details could not be clarified because of the lack of a high-resolution three-dimensional structure for hemocyanins at that time. On the other hand, Ricchelli et al. (1987) published results which were interpreted as ruling out Förster transfer as the reason for fluorescence quenching

in oxygenated hemocyanins. The later study of Boteva et al. (1993) on the fluorescence properties of hemocyanin from the tarantula *Eurypelma californicum* based its analysis on the statements made by Ricchelli et al. (1987), thereby assuming the same conclusions.

Ricchelli et al. (1987) investigated the molluscan hemocyanin of the squid *Octopus vulgaris*. They compared the fluorescence quenching elicited by three different ligands bound to the active site: O_2, CO and ANS (1-anilino-8-naphthalenesulfonate). For each of the ligands there was an overlap between the absorption spectrum of the occupied active sites and the fluorescence emission spectrum of the tryptophans. For this reason, Förster transfer should be possible in the case of all three ligands. Their calculated Förster distances R_0 and transfer efficiencies E for each ligand, computed with Eqs. (4) and (15, term on the right), respectively, are shown in Table 3 (columns 2 and 3). The results were used by them to compute an "average" donor–acceptor distance r from an inverted form of Eq. (3):

$$r = R_0 \sqrt[6]{\frac{1}{E} - 1} \tag{22}$$

These distances r should be a substitute for all donor–acceptor distances within the hemocyanin for each ligand (Table 3, column 4). These averages were identical for CO and ANS but for O_2 a much larger distance was obtained. Ricchelli et al. (1987) concluded that the quenching mechanism must be the same for the CO and ANS adduct and must be Förster transfer, but different for the O_2 complex.

The conclusions of Ricchelli et al. can be contradicted, based on a constructed model system. We assume a well-defined system with fixed donor–acceptor distances. The system may be quenched by Förster transfer. We compare the quenching in the case of two different Förster distances ($R_0 = 1.5$ nm and 2.5 nm, respectively). Our model system consists of five donors and one acceptor. The distances between the donors and the acceptor may have values of 0.5, 1, 1.5, 2 and 2.5 nm. The quenching of the donors due to Förster transfer can be calculated with Eqs. (11) and (15), yielding an averaged quantum yield and transfer efficiency, respectively, for the model system (Table 4). Based on these calculations, we continued according to the procedure of Ricchelli et al.; the distance r was calculated with Eq. (22). The results are shown in Table 4. Application of equation (22) for both model systems yields different results, even though the donor–acceptor distances are equal in both cases. In consequence, the distance r depends on the Förster distance R_0 of the system. Thus, the "average" distance r cannot be used as a substitute for all donor–acceptor distances within hemocyanin. An interpretation of different r distances for different Förster distances R_0 (due to different ligands) is not straightforward. In consequence, CO can be removed compared to the other two ligands, because it has much smaller Förster distance (Table 3). O_2 and ANS should be more or less comparable because the R_0 values are similar (Table 3). Nevertheless, there are differences in the transfer efficiencies E and distances r calculated by Ricchelli et al. This may be a consequence of the modification made in the case of ANS bound to hemocyanin: the copper ions were removed (producing apo-hemocyanin) before adding ANS, because the ligand is much more bulky than O_2 or CO. Apparently this modification of the hemocyanin had greater side effects than expected.

It seems to be coincidence that the quenching of *Octopus* hemocyanin by ANS ($E = 0.95$, Table 3) and *Eurypelma* hemocyanin by O_2 ($E = 0.92$) is almost identical. Both hemocyanins (mollusc and arthropod hemocyanin) have same active sites; however, they are different proteins with completely different primary, secondary, tertiary and quarternary structures. The number of donors (Trp) and acceptors (active sites) as well as their distances are different in arthropod and mollusc hemocyanin, according to the structures known so far (Volbeda and Hol 1989; Hazes et al. 1993; Magnus et al. 1994; Cuff et al. 1998; Perbandt et al. 2003). Thus, there is no obvious reason why the quenching in two completely different hemocyanins should be equal.

Table 3 Results of Ricchelli et al. (1987). Tryptophan fluorescence of the hemocyanin of *Octopus vulgaris* was measured as a function of the saturation binding of three different ligands to the active site: oxygen (O_2), carbon monoxide (CO) and 1-anilino-8-naphthalenesulfonic acid (ANS). On the basis of their spectroscopic data, they calculated an average Förster distance R_0, an average transfer efficiency E, and an average distance r, as described in the text

Ligand	Förster distance, R_0 (nm)	Transfer efficiency, E	"Average" distance r (nm)
O_2	2.5	0.67	2.2
CO	1.5	0.43	1.5
ANS	2.4	0.95	1.5

Table 4 The fluorescence quenching of a model system as a function of the Förster radius, R_0. The model system consists of five donors and one acceptor which quenches the donors by Förster transfer. The donor–acceptor distances selected were 0.5, 1, 1.5, 2 and 2.5 nm. The quantum yield Φ_{calc} was calculated with Eq. (11) for two different Förster radii (1.5 nm and 2.5 nm, respectively). The transfer efficiency$E$ and the "average" distance r were computed in accordance with Ricchelli et al. (1987) using Eqs. (15) and (22), respectively

Model system	Small Förster distance, R_0	Large Förster distance, R_0
Starting parameters		
Number of acceptors, A	1	1
Number of donors, D	5	5
Unquenched quantum yield, Φ_0	0.5	0.5
Förster distance, R_0(nm)	1.5	2.5
Theoretical consideration		
Quantum yield, Φ_{calc}	0.2386	0.0756
Transfer efficiency, E	0.5227	0.8487
Analog to Ricchelli et al. (1987)		
"Average" distance r (nm)	1.48	1.88

Conclusions

The paper gives a quantitative description of FRET in multi-donor multi-acceptor systems, e.g. in proteins containing more than one donor and more than one acceptor. In particular, this is shown for tarantula hemocyanin. This large respiratory protein contains 24 active sites acting as acceptors when oxygenated. It could be shown on an atomic level that the oxygenated active sites quench the fluorescence of the 148 intrinsic tryptophans by Förster transfer. The analysis shows that there are two classes of tryptophans within tarantula hemocyanin, consisting of 142 and six residues, respectively. The former class is quenched by more than 89% in the oxygenated state. The second class is quenched by less than 31%, responsible for half of the fluorescence intensity elicited of oxygenated tarantula hemocyanin. The change in the fluorescence quantum yield, although not understood, has been used for more than 20 years to investigate the cooperative oxygen binding behaviour of hemocyanins (Loewe 1978). Our results explain for the first time, on a molecular basis, why fluorescence quantum yield can be used as an intrinsic signal for the oxygen load of tarantula hemocyanin. A former study of Ricchelli et al. (1987), which seems to be in contradiction with this statement, could be disproved.

Acknowledgements We thank Hermann Hartmann for instructive discussions and the Deutsche Forschungsgemeinschaft (DFG) for financial support.

References

Baldwin MJ, Root DE, Pate JE, Fujisawa K, Kitajima N, Solomon EI (1992) Spectroscopic studies of a side-on peroxide-bridged binuclear copper(II) model complex of relevance to the active sites in oxyhemocyanin and oxytyrosinase. J Am Chem Soc 114:10421–10431

Boteva R, Ricchelli F, Sartor G, Decker H (1993) Fluorescence properties of hamocyanin from tarantula (*Eurypelma californicum*): a comparison between the whole molecule and isolated subunits. J Photochem Photobiol B 17:145–153

Burmester T (2001) Molecular evolution of the arthropod hemocyanin superfamily. Mol Biol Evol 18:184–195

Callis PR (1997) ^1L_a and ^1L_b transitions of tryptophan: applications of theory and experimental observations to fluorescence of proteins. Methods Enzymol 278:113–150

Chen RF (1967) Fluorescence quantum yields of tryptophan and tyrosine. Anal Lett 1:35–42

Cuff ME, Miller KI, van Holde KE, Hendrickson WA (1998) Crystal structure of a functional unit from *Octopus* hemocyanin. J Mol Biol 278:855–870

Decker H, Hartmann H, Sterner R, Schwarz E, Pilz I (1996) Small-angle X-ray scattering reveals differences between the quaternary structures of oxygenated and deoxygenated tarantula hemocyanin. FEBS Lett 393:226–230

De Haas F, Van Bruggen EF (1994) The interhexameric contacts in the four-hexameric hemocyanin from the tarantula *Eurypelma californicum*. A tentative mechanism for cooperative behavior. J Mol Biol 237:464–478

Dewey TG, Hammes GG (1980) Calculation of fluorescence resonance energy transfer on surfaces. Biophys J 32:1023–1036

Dos Remedios CG, Moens PDJ (1995) Fluorescence resonance energy transfer spectroscopy is a reliable "ruler" for measuring structural changes in proteins. Dispelling the problem of the unknown orientation factor. J Struct Biol 115:175–185

Fairclough RH, Cantor CR (1978) The use of singlet-singlet energy transfer to study macromolecular assemblies. Methods Enzymol 48:347–379

Floyd JS, Haralampus-Grynaviski N, Ye T, Zheng B, Simon JD, Edington MD (2001) Time-resolved spectroscopic studies of radiationless decay processes in photoexcited hemocyanins. J Phys Chem B 105:1478–1483

Förster T (1948) Zwischenmolekulare energiewanderung und fluoreszenz. Ann Phys 2:55–75

Gaykema WPJ, Hol WGJ, Vereijken JM, Soeter NM, Bak HJ, Beintema JJ (1984) 3.2 Å structure of the copper-containing, oxygen-carrying protein *Panulirus interruptus* haemocyanin. Nature 309:23–29

Hartmann H, Decker H (2002) All hierarchical levels are involved in conformational transitions of the 4×6-meric tarantula hemocyanin upon oxygenation. Biochim Biophys Acta 1601:132–137

Hazes B, Magnus KA, Bonaventura C, Bonaventura J, Dauter Z, Kalk KH, Hol WGJ (1993) Crystal structure of deoxygenated *Limulus polyphemus* subunit II hemocyanin at 2.18 Å resolution: clues for a mechanism for allosteric regulation. Protein Sci 2:597–619

Kitajima N, Fujisawa K, Moro-oka Y (1989) μ-η^2:η^2-Peroxo binuclear copper complex, (Cu(HB(3,5-iPr2pz)$_3$))2(O$_2$). J Am Chem Soc 111:8975–8976

Kitajima N, Fujisawa K, Fujimoto C, Moro-oka Y, Hashimoto S, Kitagawa T, Toriumi K, Tatsumi K, Nakamura A (1992) A new model for dioxygen binding in hemocyanin: synthesis, characterization, and molecular structure of the μ-η^2:η^2-peroxo dinuclear copper(II) complexes (Cu(HB(3,5-R2pz)$_3$))2(O$_2$) (R = i-Pr and Ph). J Am Chem Soc 114:1277–1291

Lakowicz JR (1999) Principles of fluorescence spectroscopy, 2nd edn. Kluwer/Plenum, New York

Linzen B, Soeter NM, Riggs AF, Schneider HJ, Schartau W, Moore MD, Yokota E, Behrens PQ, Nakashima H, Takagi T, Nemoto T, Vereijken JM, Bak HJ, Beintema JJ, Volbeda A, Gaykema WPJ, Hol WGJ (1985) The structure of arthropod hemocyanins. Science 229:519–524

Loewe R (1978) Hemocyanins in spiders V: fluorimetric recording of oxygen binding curves, and its application to the analysis of allosteric interactions in *Eurypelma californicum* hemocyanin. J Comp Physiol 128:161–168

Magnus KA, Hazes B, Ton-That H, Bonaventura C, Bonaventura J, Hol WG (1994) Crystallographic analysis of oxygenated and deoxygenated states of arthropod hemocyanin shows unusual differences. Proteins 19:302–309

Markl J, Decker H (1992) Molecular structure of the arthropod hemocyanins. Adv Comp Environ Physiol 13:325–375

Markl J, Kempter B, Linzen B, Bijholt MMC, Van Bruggen EFJ (1981) Hemocyanins in spiders, XVI[1]. Subunit topography and a model of the quaternary structure of *Eurypelma* hemocyanin. Hoppe Seylers Z Physiol Chem 362:1631–1641

Perbandt M, Guthohrlein E W, Rypniewski W, Idakieva K, Stoeva S, Voelter W, Genov N, Betzel C (2003) The structure of a functional unit from the wall of a gastropod hemocyanin offers a possible mechanism for cooperativity. Biochemistry 42:6341–6346

Ricchelli F, Beltramini M, Flamigni L, Salvato B (1987) Emission quenching mechanisms in *Octopus vulgaris* hemocyanin: steady state and time-resolved fluorescence studies. Biochemistry 26:6933–6939

Richey B, Decker H, Gill SJ (1983) A direct test of the linearity between optical density change and oxygen binding in hemocyanins. In: Wood EJ (ed) Life chemistry reports: supplement 1. Harwood, New York, pp 309–312

Salvato B, Beltramini M (1987) Hemocyanins: molecular structure and reactivity of the binuclear copper site. Life Chem Rep 5:249–275

Salvato B, Beltramini M (1990) Hemocyanins: molecular architecture, structure and reactivity of the binuclear copper active site. Life Chem Rep 8:1–47

Savel-Niemann A, Markl J, Linzen B (1988) Hemocyanins in spiders. XXII. Range of allosteric interaction in a four-hexamer hemocyanin. Co-operativity and Bohr effect in dissociation intermediates. J Mol Biol 204:385–395

Shaklai N, Daniel E (1970) Fluorescence properties of hemocyanin from *Levantina hierosolima*. Biochemistry 9:564–568

Shaklai N, Daniel E (1972) Phosphorescence properties of hemocyanin from *Levantina hierosolima*. Biochemistry 11:2199–2203

Stryer L (1978) Fluorescence energy transfer as a spectroscopic ruler. Annu Rev Biochem 47:819–846

Van der Meer BW, Coker G, Chen SYS (1994) Resonance energy transfer. VCH, New York

Van Heel M, Dube P (1994) Quaternary structure of multihexameric arthropod hemocyanins. Micron 25:387–418

Van Holde KE, Miller KI (1995) Hemocyanins. Adv Protein Chem 47:1–81

Van Holde KE, Miller KI, Decker H (2001) Hemocyanins and invertebrate evolution. J Biol Chem 276:15563–15566

Voit R, Feldmaier-Fuchs G, Schweikardt T, Decker H, Burmester T (2000) Complete sequence of the 24-mer hemocyanin of the tarantula *Eurypelma californicum*. Structure and intramolecular evolution of the subunits. J Biol Chem 275:39339–39344

Volbeda A, Hol WG (1989) Crystal structure of hexameric haemocyanin from *Panulirus interruptus* refined at 3.2 Å resolution. J Mol Biol 209:249–279